JP1.10

NUMERICAL PREDICTION OF HEAT ISLAND MITIGATION EFFECT ON DECREASE IN AIR TEMPERATURE IN TOKYO

Hidetoshi Tamura*, Koichiro Ishii**, Hitoshi Yokoyama**, Tetsusiro Iwatsubo*,
Hiromaru Hirakuchi*, Haruo Ando**, Takako Yamaguchi**,Takehiko Mikami***,
Mika Ichino** and Yukari Akiyama**

* Central Research Institute of Electric Power Industry
** Tokyo Metropolitan Research Institute for Environmental Protection
*** Tokyo Metropolitan University

1. INTRODUCTION

The intensity of urban heat island is known to be stronger as city size (for example population of city) (Oke, 1973). In Tokyo 23 wards (hereinafter referred to as "Tokyo") with more than eight million people, urban heat island phenomenon is actualized and feared as a factor of increase in heatstroke patients and raising cooling energy consumption in summer. Therefore, Tokyo Metropolitan Government promotes some heat island mitigation measures concerning with urban greening, reducing anthropogenic heat, and so on.

In introducing heat island mitigation measures, it is important to grasp these faculties in advance. A three dimensional numerical simulation is thought to be one of the most effective tools for this purpose. In previous studies, three-dimensional numerical simulations have been performed in order to predict the contribution of some influential factors like land coverage or anthropogenic heat to urban heat island (Kimura and Takahashi, 1991). By using a three-dimensional numerical simulation with the horizontal distribution of surface coverage and anthropogenic heat, the effect of mitigation measures on decrease air temperature can be evaluated with their various spatial arrangement patterns in urban area. On the other hand, it is required to pay attention to the adequacy of numerical model by comparing its results with field observation data.

* ***Corresponding author address:*** Hidetoshi TAMURA, Central Research Institute of Electric Power Industry, 1646 Abiko, Abiko-shi, Chiba-ken 270-1194, JAPAN; e-mail: tamtam@criepi.denken.or.jp

In this study, firstly, a three-dimensional numerical simulation model is compared with field observation data, and secondly, the model is applied to Tokyo in order to estimate the effect of heat island mitigation measures concerning with urban greening, water retentive pavement, high light-reflective paint, and reducing anthropogenic heat on decrease in air temperature. Here, the amount of these mitigation measures with their spatial distribution is determined as these expected values in 2030.

2. NUMERICAL MODEL

A three-dimensional numerical simulation model used in this study is developed by authors. The basic equations are in **Table-1**, and the schematic image of the model is shown in **Figure-1**, respectively. The model is composed of two parts. The one is the 'atmospheric model' and the other is the 'surface model'.

In the atmospheric model, atmospheric temperature, specific humidity, and three-dimensional wind velocities are calculated unsteadily by finite-difference-methods with the hydrostatic and Bousinesq approximation. The horizontal resolution of the model is one or a few kilometers. The basic equations are the equation (1)-(6) in **Table-1**.

In the surface model, the heat transfer to atmosphere is calculated under the influence of solar radiation, atmospheric radiation, and anthropogenic heat. Surface temperature is calculated from heat balance equation shown in the equation (7). The effect of heat storage into surface materials is considered with heat conductive equation in the equation (8). In this surface model, it is possible to calculate the heat

Table 1 Basic equations of numerical model

Equations in atmosphere

$$\frac{\partial hu}{\partial t}+\frac{\partial huu}{\partial x}+\frac{\partial huv}{\partial y}+\frac{\partial huw^*}{\partial z^*}=fhv-h\theta\frac{\partial \pi'}{\partial x}+gh\frac{\theta'}{\theta-\theta'}\frac{z_T-z^*}{z_T}\frac{\partial z_G}{\partial x}+\frac{\partial}{\partial x}\left(hK_{Hm}\frac{\partial u}{\partial x}\right)+\frac{\partial}{\partial y}\left(hK_{Hm}\frac{\partial u}{\partial y}\right)+\frac{z_T^{\,2}}{h}\frac{\partial}{\partial z^*}\left(K_{Vm}\frac{\partial u}{\partial z^*}\right) \quad (1)$$

$$\frac{\partial hv}{\partial t}+\frac{\partial hvu}{\partial x}+\frac{\partial hvv}{\partial y}+\frac{\partial hvw^*}{\partial z^*}=-fhu-h\theta\frac{\partial \pi'}{\partial y}+gh\frac{\theta'}{\theta-\theta'}\frac{z_T-z^*}{z_T}\frac{\partial z_G}{\partial y}+\frac{\partial}{\partial x}\left(hK_{Hm}\frac{\partial v}{\partial x}\right)+\frac{\partial}{\partial y}\left(hK_{Hm}\frac{\partial v}{\partial y}\right)+\frac{z_T^{\,2}}{h}\frac{\partial}{\partial z^*}\left(K_{Vm}\frac{\partial v}{\partial z^*}\right) \quad (2)$$

$$\frac{\partial \pi'}{\partial z^*}=\frac{h}{z_T}\frac{g\theta'}{(\theta-\theta')^2} \quad (3) \qquad \frac{\partial hu}{\partial x}+\frac{\partial hv}{\partial y}+\frac{\partial hw^*}{\partial z^*}=0 \quad (4)$$

$$\frac{\partial h\theta'}{\partial t}+\frac{\partial h\theta' u}{\partial x}+\frac{\partial h\theta' v}{\partial y}+\frac{\partial h\theta' w^*}{\partial z^*}=\frac{\partial}{\partial x}\left(hK_{Hh}\frac{\partial \theta'}{\partial x}\right)+\frac{\partial}{\partial y}\left(hK_{Hh}\frac{\partial \theta'}{\partial y}\right)+\frac{z_T^{\,2}}{h}\frac{\partial}{\partial z^*}\left(K_{Vh}\frac{\partial \theta'}{\partial z^*}\right)+\frac{Q}{\rho c_p} \quad (5)$$

$$\frac{\partial hq}{\partial t}+\frac{\partial hqu}{\partial x}+\frac{\partial hqv}{\partial y}+\frac{\partial hqw^*}{\partial z^*}=\frac{\partial}{\partial x}\left(hK_{Hh}\frac{\partial q}{\partial x}\right)+\frac{\partial}{\partial y}\left(hK_{Hh}\frac{\partial q}{\partial y}\right)+\frac{z_T^{\,2}}{h}\frac{\partial}{\partial z^*}\left(K_{Vh}\frac{\partial q}{\partial z^*}\right)+\frac{M}{\rho} \quad (6)$$

Equations at and into surface

$$c_t\frac{\partial T_s}{\partial t}=\{(1-\alpha)\cdot\tau\cdot S_d+(L_d-L_u)\}-H-lE-S \quad (7) \qquad \frac{\partial T_g}{\partial t}=\frac{k_g}{\rho_g c_g}\frac{\partial^2 T_g}{\partial z_g^{\,2}} \quad (8)$$

Equations for urban canopy

$$V_{(h)}=\frac{u_{(a)}}{\kappa}\Psi_{M(a)}(h_b-d) \quad (9) \qquad V_{(c)}=V_{(h)}\sqrt{\frac{\exp(0.5Ch_b)-\exp(-0.5Ch_b)}{\exp(Ch_b)-\exp(-Ch_b)}} \quad (10)$$

$$H_{(ra)}=\rho_a c_a\frac{\kappa^2 V_{(a)}}{\Psi_{M(ra)}\Psi_{H(ra)}}\left(T_{s(r)}-\theta_{(a)}\right)+Q_{(ra)} \quad (11) \qquad H_{(wc)}=\rho_a c_a\left(0.01\sqrt{\frac{V_{(c)}}{W_1}}\right)\left(T_{s(w)}-\theta_{(c)}\right)+Q_{(wc)} \quad (12)$$

$$H_{(gc)}=\rho_a c_a\frac{\kappa^2 V_{(c)}}{\Psi_{M(gc)}\Psi_{H(gc)}}\left(T_{s(g)}-\theta_{(c)}\right)+Q_{(gc)} \quad (13)$$

$$(W_2^{\,2}+2W_1W_2)H_{(ca)}=(W_2^{\,2}+2W_1W_2)H_{(gc)}+4W_1h_bH_{(wc)} \quad (14) \qquad H_{(ca)}=C_f\rho_a c_a\left(\frac{V_{(h)}+V_{(c)}}{2}\right)\left(\theta_{(c)}-\theta_{(a)}\right) \quad (15)$$

C : drag coefficient of building
C_f : heat exchange coefficient between urban canopy layer and upper surface layer
c_g : heat capacity of ground or urban canopy materials
c_t : $= (86400\rho_g c_g k_g / 4\pi)^{0.5}$
c_p : heat capacity of air
d : zero-plane displacement
E : moisture flux to atmosphere
f : coriolis parameter
g : acceleration of gravity
H : sensible heat budget
h : $= z_T - z_G$
h_b : hight of buildings
K_{Hh} : horizontal eddy diffusivity
K_{Vh} : vertical eddy diffusivity
K_{Hm} : horizontal eddy viscosity
K_{Vm} : vertical eddy viscosity

k_g : heat conductivity into ground or urban canopy materials
L_d : downward long wave radiation flux at ground level
L_u : upward long wave radiation flux at ground level
l : heat of vaporizarion
M : anthropogenic latent heat
Q : anthropogenic sensible heat
q : specific humidity
S : heat budget into ground
S_d : solar radiation in upper
T_g : temperature into ground or urban canopy materials
T_s : temperature at surface of ground or urban canopy materials
u : eastward wind velocity
v : northward wind velocity

V : wind velocity
u_* : frictional velocity
W_1 : width of buildings
W_2 : interval of buildings
w_* : vertical wind speed in coordinate
z_G : hight of ground
z_T : hight of top layer of atmosphere
z_g : depth into materials
z_* : terrain coordinate
α : surface albedo
κ : von Karman coefficient
π' : exner function
θ : potential temperature
θ' : difference of temperatue from its standard value
ρ_a : density of air
ρ_g : density of ground or urban canopy materials

τ : atmospheric transmissivity
Ψ_H : integrated universal function for heat
Ψ_M : integrated universal function for momentum

Suffixes in a parenthes means a location of parameters
(a): lowest layer of atmosphric model
(h): top of building hight
(c): in a ravine of buildings
(g): road surface
(r): roof surface
(w): wall surface

(AB): between (A) and (B)

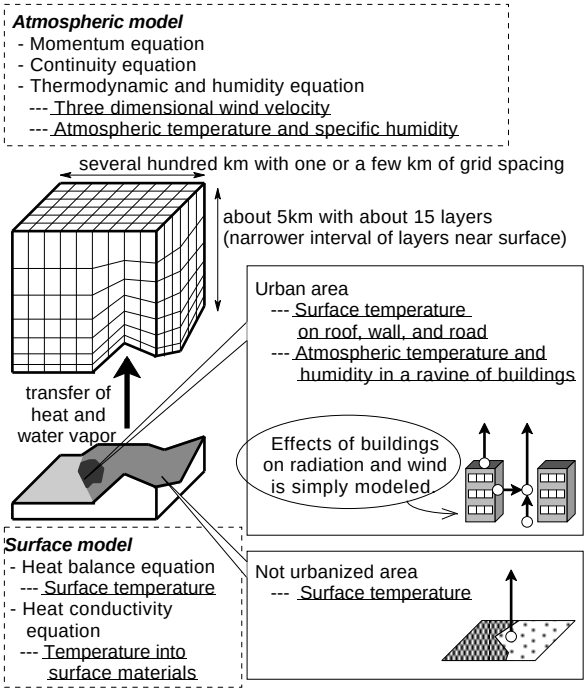

Figure-1 A scematic image of numerical simulation model (underlied text means the parameters to be predicted)

budget by finer horizontal resolution than the atmospheric model by bundling up the heat budgets belong to same atmospheric grid.

Furthermore, a simplified urban canopy model is adopted for urban surface modeling in order to consider the effect of buildings on radiation and wind velocity. The principal equations of the urban canopy model are the equation (9)-(12). In this urban canopy model, the surface temperatures of roof, wall, and road are predicted, respectively. Furthermore, the air temperature in a ravine of buildings (hereinafter referred to as "surface air temperature") can be predicted. The needed numerical parameters for geometric pattern of buildings are height, width, and interval of buildings averaged in each horizontal numerical grid. In non-urban area, on the other hand, land surface is regarded as a plane and a roughness model is applied.

3. COMPARISON OF NUMERICAL RESULTS WITH FIELD DATA

3.1 Field data

In order to evaluate the numerical model, we use the

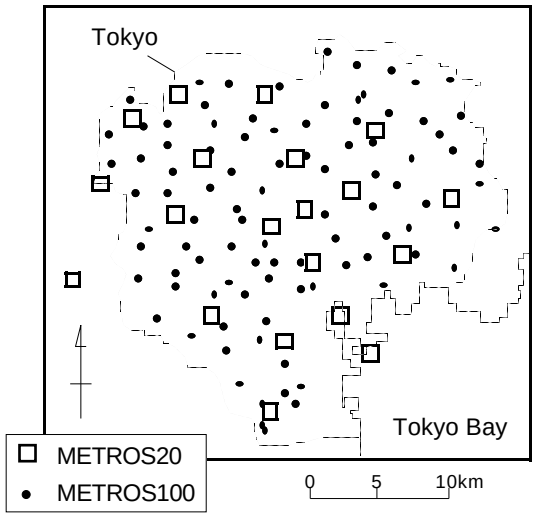

Figure-2 The observation points of METROS

field observation data with METROS (Metropolitan Environmental Temperature and Rainfall Observation System) set up by Tokyo Metropolitan Research Institute for Environmental Protection and Tokyo Metropolitan University (Mikami et al., 2003). The distribution of observation points is shown in **Figure-2**. METROS20 is a system to observe air temperature, relative humidity, wind velocity, wind direction, air pressure, and rainfall at 20 points of the top of buildings in Tokyo. METROS100 is to observe air temperature and relative humidity at 100 points of 1.5m height of ground level in Tokyo.

The effectiveness of METROS is to have high-density continuous observation points. Especially for air temperature and relative humidity just above ground level, METROS has 100 observation points over Tokyo (61500 ha). The METROS data with such high resolution can grasp the horizontal distribution of temperature over Tokyo in detail.

3.2 Numerical condition

In this study, a numerical simulation of the model is carried out on a typical summer day of August 29, 2002. The meteorological conditions of solar radiation and the vertical profile of air temperature and humidity are needed for simulation. Here, these data are obtained from the observation data by Japan Meteorological Agency.

The horizontal domain of simulation is 388 km from

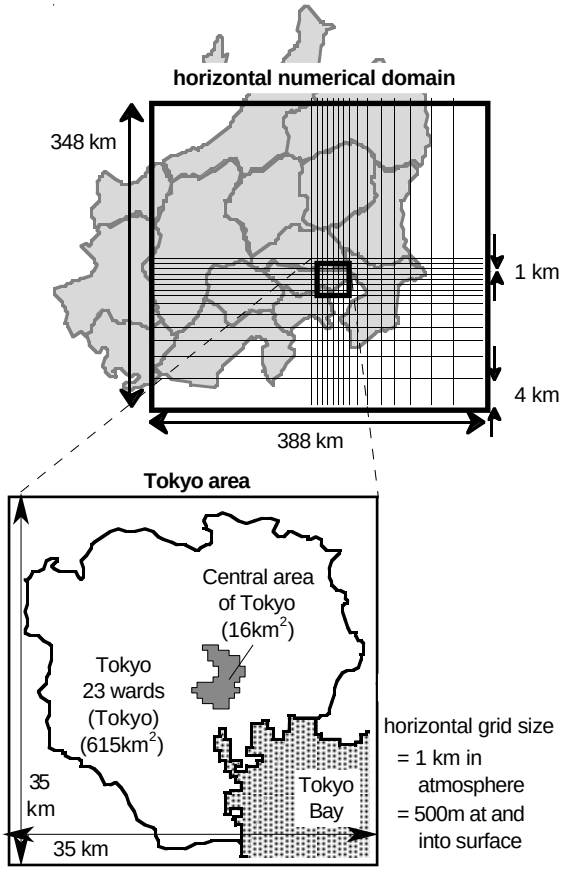

Figure-3 The horizontal numerical domain

west to east and 348 km from south to north, respectively (see in **Figure-3**). A variable mesh is used in the horizontal area. In the area of 35km*35km includes Tokyo (shown in **Figure-2)**, horizontal grid size is 1km in atmosphere and 0.5km at surface. In the fringe of horizontal domain, the grid size becomes broader from 1km to 4km with distance from Tokyo.

In each surface grid, it is needed to set parameters to characterize surface properties. Here, altitude and surface coverage (occupancy ratio of sea, forest, grass, urban, and so on) are set up from GIS data by Geographical Survey Institute of Japan. In addition, geometry of buildings for the urban canopy model and anthropogenic heat are estimated similarly with GIS data by Tokyo Metropolis and Road Traffic Census data by Ministry of Land Infrastructure and Transport. As for anthropogenic heat data, they are set up as time-varying values in two forms, namely, sensible heat and latent heat.

3.3 Results

Numerical simulation of the model is compared with METROS data in a typical summer day of August 29, 2002. The distribution of horizontal wind velocity at three symbolic points of time is shown in **Figure-4** for numerical simulation and field data by METROS20. In numerical results, wind velocity is small at 06:00; sea breeze toward NNW-ward can be seen at 14:00; and wind direction changes into NNE-ward at 20:00. The same features can be seen in field data.

For temperature, on the other hand, **Figure-5** is distribution of surface air temperature for numerical simulation and field data by METRO100. In numerical results, the highest temperature reveals in center of Tokyo at 06:00, NW-ward of center of Tokyo at 14:00, and northward of center of Tokyo at 20:00. These results concern wind direction (see **Figure-4**), that is, the leeward of center of Tokyo becomes hotter. The same features can be seen in field data.

From the comparison mentioned above, we confirmed that the numerical results are in good agreement with the observation of horizontal distribution of air temperature, wind velocity, and wind direction near the surface.

4. ESTIMATION OF EVAPORATION EFFICIENCY FOR MITIGATION MEASURES

In order to estimate the effect of heat island mitigation measures by numerical simulation, it is needed to determine the surface physical parameters for roof greening and water retentive pavement. The evaporation efficiency, which is one of the important surface parameters, is estimated from the surface heat budget field data of roof greening and water retentive pavement observed by Tokyo Metropolitan Research Institute for Environmental Protection (Yokoyama et al., 2004) and Institute of Civil Engineering of Tokyo Metropolitan Government (Minegishi et al., 2002), respectively. For this estimation, the urban canopy model is picked out from the three-dimensional model and used as a vertical column model in order to evaluate surface heat balance. Meteorological conditions of wind velocity, air temperature and air humidity just upon urban canopy layer is set up from the field-measured data. The parameter values of the evaporation efficiency for

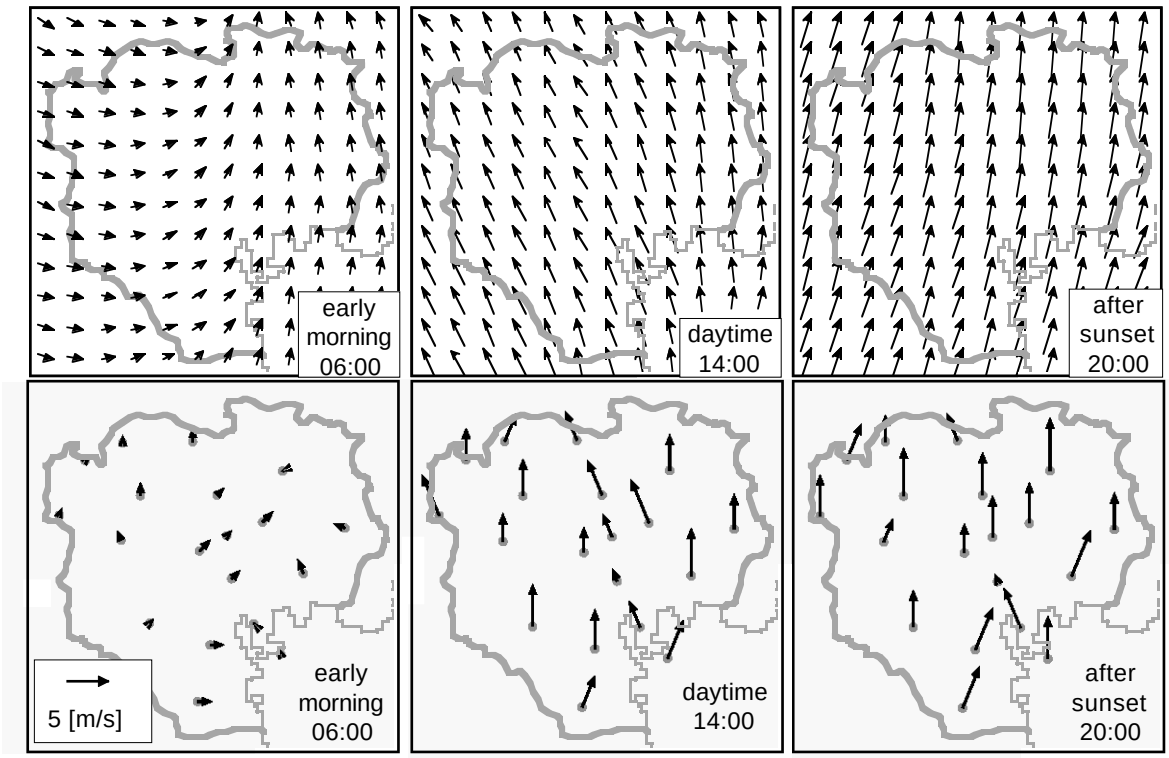

Figure-4 The simulated wind velocity at 45m height (upper three figures) and the wind velocity measured by METRS20 converted into 45m height by an exponential function (lower three figures) at 6:00, 14:00, and 20:00

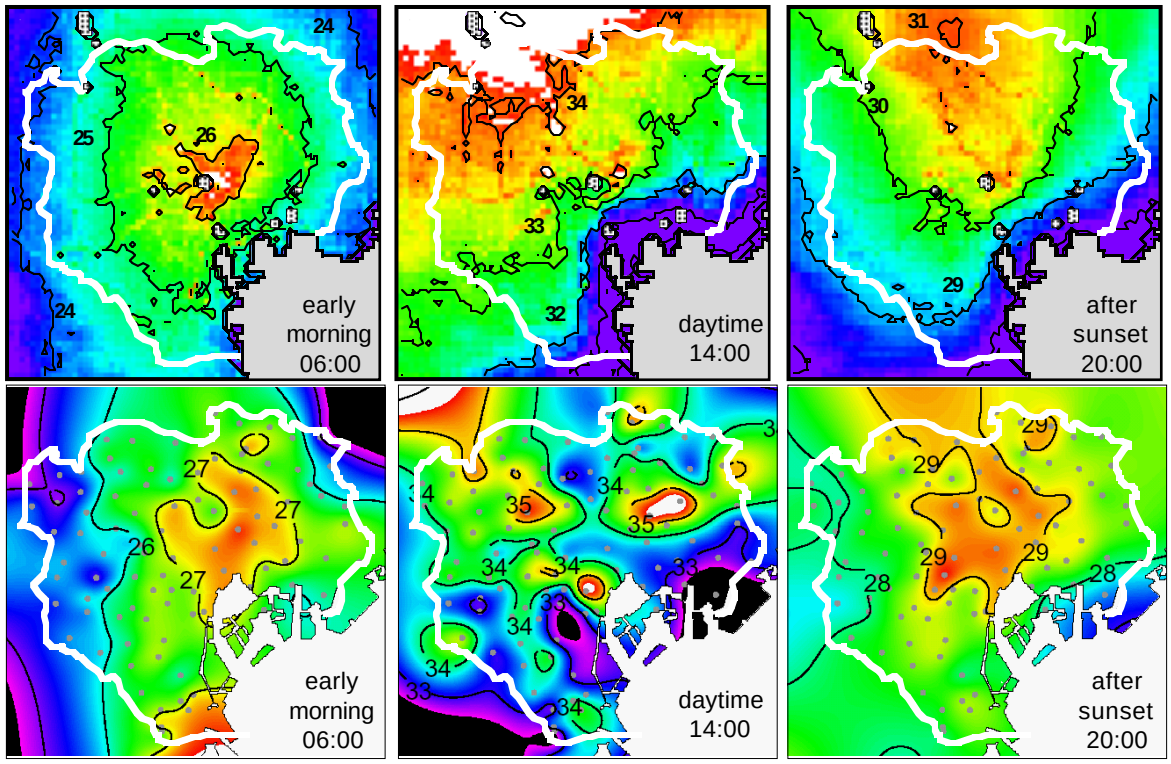

Figure-5 The simulated surface air temperature (upper three figures) and the air temperature measured at 1.5m height by METROS100 (lower three figures) at 6:00, 14:00, and 20:00

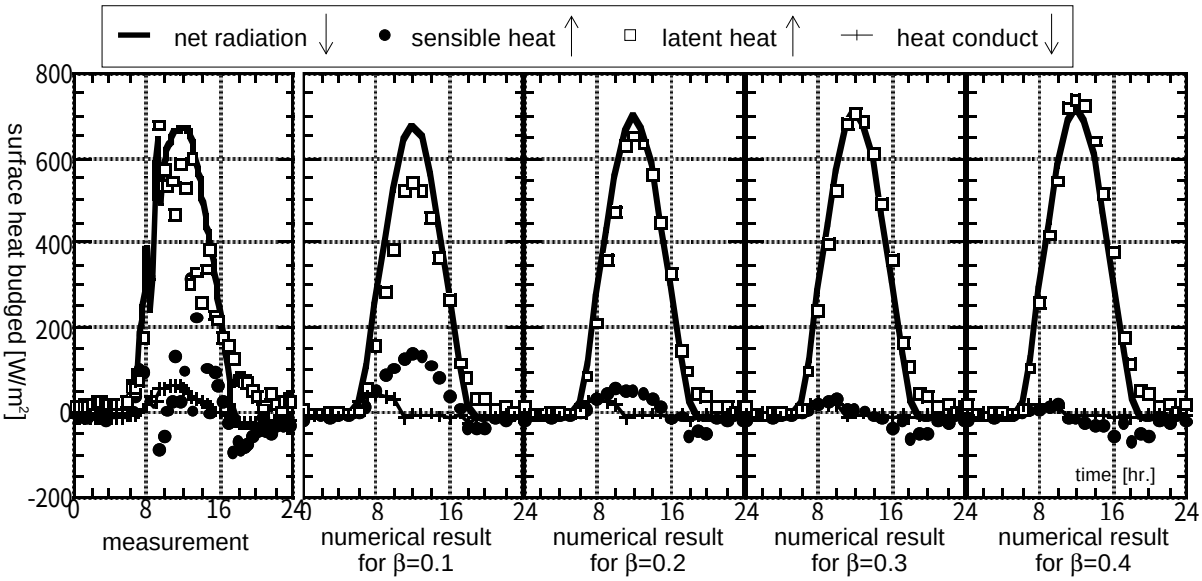

Figure-6 The surface heat balance on a roof greening area measured on 25 August 2003, and numerical results of four cases with different value of evaporation efficiency by using vertical column model

roof greening and water retentive pavement are estimated by trial and error comparing with the model and the above observation heat budgets.

As the example of estimation for roof greening, surface heat balance is shown in **Figure-6** for a field measurement and four numerical cases with different value of the evaporation efficiency. In this case, the evaporation efficiency of roof greening is presumed about 0.2. Similarly, the evaporation efficiency of water retentive pavement is presumed about 0.05.

5. NUMERICAL PREDICTION OF MITIGATION EFFECTS

5.1 Mitigation

Finally, the effect of heat island mitigation measures on decreasing in temperature is estimated by the three-dimensional numerical simulation. Here, a mitigation scenario is supposed by introducing five kinds of mitigation measures mentioned below, simultaneously.

1) Introducing roof greening into 45.0% of roof area of buildings with over 1000 square meters of a building site and greening into 4.4% of urban ground surface in Tokyo
2) Introducing water retentive pavement into 29% of road in central area of Tokyo (see **Figure-3**)
3) Introducing high light-reflective paint into 20% of building roofs in Tokyo
4) Decrease in 41.5% of anthropogenic heat from automobiles in Tokyo by improvement of fuel cost and increase in travel speed of cars
5) Decrease in 21.5% of anthropogenic heat of houses and 26.5% of buildings for business use in Tokyo by improvement of thermal insulation efficiency of buildings and improvement of system for energy conservation

The numerical values for these mitigation measures are set up as expected values for Tokyo in 2030. The distribution of each measure is shown in **Figure-7**.

5.2 Results

Another numerical simulation in a typical summer day condition (August 29, 2002) is carried out, but with the future condition after mitigation measures in 2030. The difference between two numerical results with and without the five measures mentioned above reveals the effect of these measures.

The surface air temperatures of two cases without and with mitigations are shown in **Figure-8** with the temperature difference between these two cases. Decrease in the area-averaged temperature over Tokyo (61500ha) is predicted to be about 0.5K in daytime, and 0.2K in nighttime, respectively. In

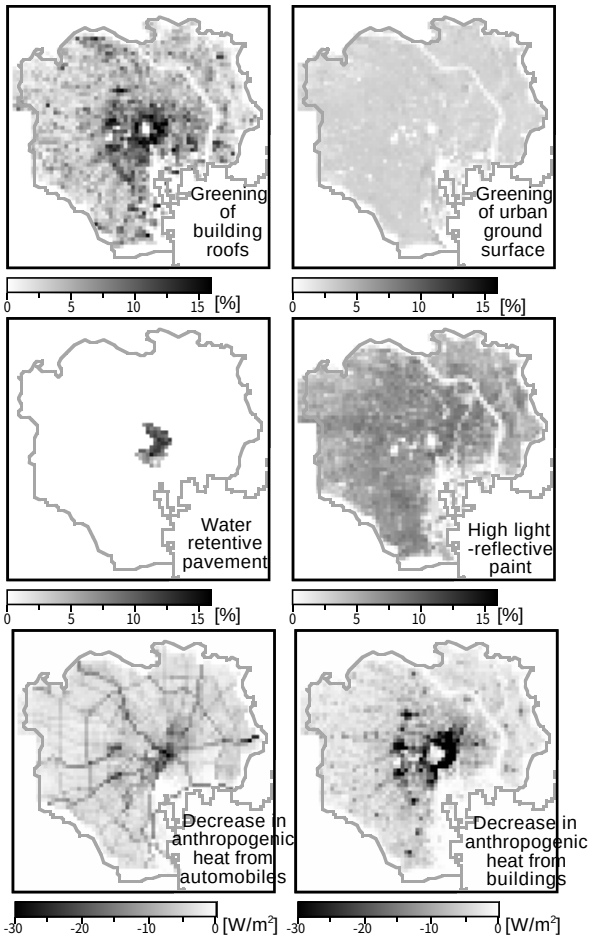

Figure-7 The distribution of each mitigation meaasure

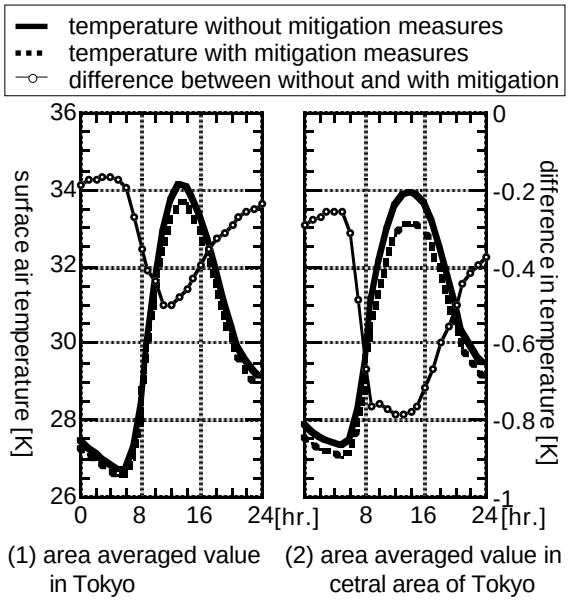

Figure-8 The time series of surface air temperature and its difference between with and without heat island mitigation measures

central area of Tokyo (1600ha), on the other hand, temperature decrease is predicted to be about 0.8K in daytime.

Horizontal distribution of change in surface air temperature at 6:00, 14:00, and 20:00 is shown in **Figure-9**. It is clear that the decrease in temperature is large in central area of Tokyo. In addition, temperature decrease is noticeable in the leeward of central area of Tokyo (see **Figure-4**). This is thought to be a phenomenon caused by decreasing the heat advection from central area of Tokyo.

Furthermore, numerical cases for introducing each mitigation measure mentioned above are carried out. The difference between two numerical results with and without each measure at 14:00 is shown in **Table-2**. In the scenario of this study, urban greening shows the largest value in decrease in surface air temperature. In central area of Tokyo, the effect of measures related to decreasing anthropogenic heat are seems to be large.

6. CONCLUSIONS

The three-dimensional numerical simulation is carried out in order to estimate the effect of heat island mitigation measures on decrease in air temperature in Tokyo. Here, mitigation measures are assumed concerning with urban greening, water retentive pavement, high light-reflective paint, and reducing anthropogenic heat. The amount of these measures is assumed as expected values for Tokyo in 2030. In daytime, decrease in area-averaged air temperature is predicted about 0.5K over Tokyo and 0.8K over central area of Tokyo. Furthermore, it is found that the remarkable decrease in temperature reveals on the leeward of central Tokyo.

In this study, the simulation is carried out under a very calm meteorological condition. The evaluation of measures under various wind condition is remained as future work.

REFERENCES

Kimura, F. and Takahashi, S., 199: The Effects of

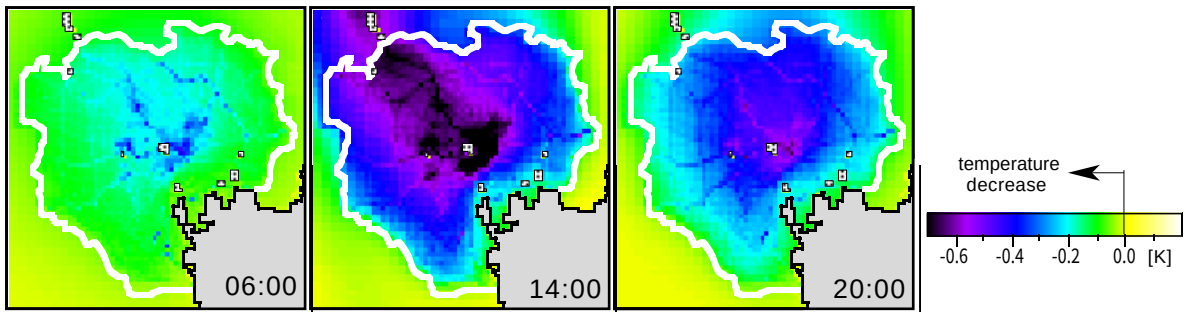

Figure-9 The horizontal distribution of change in surface air temperature by introducing heat island mitigation measures

Table-2 The effect of each mitigation measure on decrease in surface air temperature

mitigation	Area averaged value in Tokyo		Area averaged value in central area of Tokyo	
	introduction ratio *	difference in temperature	introduction ratio *	difference in temperature
(1) Urban greening	6.5 %	-0.20 K	13.5 %	-0.24 K
(2) Water retentive pavement	0.2 %	-0.01 K	8.8 %	-0.15 K
(3) High light-refrective paint	5.1 %	-0.09 K	6.6 %	-0.09 K
(4) Decrease in anthropogenic heat from automobile	41.5 %	-0.08 K	41.0 %	-0.15 K
(5) Decrease in anthropogenic heat from buildings	20.4 %	-0.06 K	25.4 %	-0.14 K

* Here, the 'introduction ratio' means the ratio of introduced area to all objective area for (1),(2), and (3), and the ratio of decrease in anthropogenic heat to total anthropogenic heat for (4) and (5).

land-use and anthropogenic heating on the surface temperature in the Tokyo metropolitan area: A numerical experiment, ***Atmospheric Environment***, Vol.25B, No.2, pp.155-164.

Mikami, T., Ando, H., Morishima, W., Izumi, T., and Shinoda, T., 2003: A new urban heat island monitoring system in Tokyo, ***Proceedings of Fifth International Conference on Urban Climate***, O.3.5

Minegishi, J., Kobayashi, K., Ohmi, J. and Abe, T., 2002: A study of reduction function of surface temperature of the water-absorptive pavement, ***Annual Report I.C.E. of TMG 2002***, pp.53-64. (in Japanese)

Oke, T.R., 1973: City size and the urban heat island, ***Atmospheric Environment***, Vol.7, pp.769-779.

Yokoyama, H., Yamaguchi, T., and Ishii, K., 2004: Study of mitigation the urban heat islands by light and thin rooftop greening, ***Annual Report of the Tokyo Metropolitan Research Institute for Environmental Protection 2004***, pp.3-10. (in Japanese)